Nonergodicity in the Anisotropic Dicke Model

Wouter Buijsman,[1,*] Vladimir Gritsev,[1] and Rudolf Sprik[2]
[1]Institute for Theoretical Physics Amsterdam and Delta Institute for Theoretical Physics, University of Amsterdam, Science Park 904, 1098 XH Amsterdam, The Netherlands
[2]Van der Waals-Zeeman Institute, University of Amsterdam, Science Park 904, 1098 XH Amsterdam, The Netherlands
(Received 21 October 2016; published 23 February 2017)

We study the ergodic-nonergodic transition in a generalized Dicke model with independent corotating and counterrotating light-matter coupling terms. By studying level statistics, the average ratio of consecutive level spacings, and the quantum butterfly effect (out-of-time correlation) as a dynamical probe, we show that the ergodic-nonergodic transition in the Dicke model is a consequence of the proximity to the integrable limit of the model when one of the couplings is set to zero. This can be interpreted as a hint for the existence of a quantum analogue of the classical Kolmogorov-Arnold-Moser theorem. In addition, we show that there is no intrinsic relation between the ergodic-nonergodic transition and the precursors of the normal-superradiant quantum phase transition.

DOI: 10.1103/PhysRevLett.118.080601

Nonergodic quantum dynamics and, more generally, nonergodic phases of quantum many-body systems have recently attracted great interest in the condensed matter community [1–4]. One of the paradigmatic subclasses of these systems is provided by integrable models of quantum many-body systems, such as the anisotropic Heisenberg (XXZ) spin-$1/2$ chain [5], the one-dimensional Hubbard model [6], central spin models [7], as well as various other interacting one-dimensional bosonic [8] or fermionic [9] models. While integrable systems are characterized by an infinite number of integrals of motion leading to nonergodic dynamics, they do not exhaust all possible nonergodic phases. In fact, many-body localized systems represent a new class of nonergodic phases with the ergodic-nonergodic transition (ENET) driven by disorder strength [2,10]. For these systems, dynamically emergent conserved quantities are responsible for a variety of distinctive properties of many-body localized phases. Nonergodic phases could also exist in driven and dissipative quantum systems [11,12]. The existence of nonergodic phases breaking traditional statistical physics by not satisfying the eigenstate thermalization hypothesis [13] can possibly be linked with the existence of a yet unknown quantum version of the classical Kolmogorov-Arnold-Moser theorem [14,15] (qualitatively stating that classical integrable systems remain quasi-integrable under weak perturbations). Despite several attempts to identify such a quantum theorem [3,16–18], fundamental questions are still open, and progress mostly lies in the observation of indirect signatures in specific models.

Here, we discuss the emergence of extended nonergodic phases in a generalized version of the Dicke model [19]. This model has two independent light-matter coupling constants, corresponding to the corotating and counterrotating terms in the Hamiltonian. The model can be derived as an effective model starting from three- or four-level emitter schemes [20,21]. While it is Bethe ansatz integrable when one of the couplings is zero (then representing a variant of the Gaudin model [22]), tuning the coupling parameter from a nonzero value and considering it as a perturbation allows us to study the transition from the nonergodic phase (corresponding to quasi-integrability) to the ergodic phase (associated with quantum chaotic behavior). First, we show that this transition occurs at finite values of the integrability-breaking parameter, with the nonergodic phase occupying an extended region of the phase diagram. Interestingly, this effect can be observed experimentally [23,24]. Second, we show that there is a clear difference between the ENET and the precursors of the normal-superradiant quantum phase transition [25], thereby shining new light on the question whether ENETs and normal-superradiant quantum phase transitions can be intrinsically related [26–28].

The Dicke model is a paradigmatic model to benchmark tools detecting quantum chaos [28–31]. Here, we use several complementary methods to detect the ENET: we study the level statistics, the average ratio of consecutive level spacings, and the quantum butterfly effect. All of these methods are complementary, while indicating the same shape of the ENET. We note that in these and many other studies in the past, signatures of nonergodic behavior were quantified by quantities related to eigenvalues and eigenfunctions. However, in the present many-body context we emphasize the need of *dynamical* probes of nonergodicity. The quantum butterfly effect (also known as "scrambling" or "out-of-time correlation") [32–36] serves this purpose for us. This recently developed tool has been used, for example, in quantum gravity [36], black hole physics [32], and many-body localization [37]. To our knowledge, its use in quantifying the phase diagram of a quantum optical system is new.

Anisotropic Dicke model.—We consider the anisotropic Dicke model (ADM),

$$H = \omega a^\dagger a + \omega_0 J_z + \frac{g_1}{\sqrt{2j}}(a^\dagger J_- + a J_+) + \frac{g_2}{\sqrt{2j}}(a^\dagger J_+ + a J_-), \quad (1)$$

where a, $a^\dagger$ are bosonic (cavity mode) operators satisfying $[a, a^\dagger] = 1$ in units $\hbar = 1$ and $J_{\pm,z} = \sum_{i=1}^{2j} \frac{1}{2}\sigma_{\pm,z}^{(i)}$ are angular momentum operators of a pseudospin with length j composed of $N = 2j$ noninteracting spin-1/2 atoms described by the Pauli matrices $\sigma_{\pm,z}^{(i)}$ acting on site i. In the following, we work in the basis $\{|n\rangle \otimes |j, m\rangle\}$ with $a^\dagger a|n\rangle = n|n\rangle$ and $J_z|j, m\rangle = m|j, m\rangle$. The ADM describes the interaction between a single-mode bosonic field with frequency ω and the atoms with level splitting ω_0, within the dipole approximation coupled to the field with coupling parameters g_1 and g_2 for the corotating and counterrotating terms, respectively. Several experimental realizations of the ADM have been proposed [20,24,38,39]. For $g_1 = g_2 = g$, the ADM reduces to the Dicke model with coupling parameter g. The ADM possess a parity symmetry $[H, \Pi] = 0$ with $\Pi = \exp(i\pi[a^\dagger a + J_z + j])$ having eigenvalues ± 1. Here, the focus is restricted to the positive parity subspace, which includes the ground state for the parameter ranges considered in this Letter (verified numerically). When applying the rotating-wave approximation, i.e., setting $g_2 = 0$, the total number of excitations $n + m + j$ is conserved, making the ADM Bethe ansatz integrable [22]. By rotating $J_y \to -J_y$, $J_z \to -J_z$ and setting $\omega_0 \to -\omega_0$, the ADM with $g_1 = 0$ maps onto the ADM with $g_2 = 0$, showing that the ADM is integrable for $g_1 = 0$ or $g_2 = 0$. In the thermodynamic limit $j \to \infty$, the ADM exhibits a second-order quantum phase transition [40] at $g_1 + g_2 = \sqrt{\omega\omega_0}$ with order parameter $a^\dagger a/j$, separating the normal phase at $g_1 + g_2 < \sqrt{\omega\omega_0}$ with $\langle a^\dagger a\rangle/j = 0$ from the superradiant phase with $\langle a^\dagger a\rangle/j = \mathcal{O}(1)$. For finite j, it has been shown numerically that the Dicke model displays a transition from nonergodic to ergodic behavior with an increasing value of g at $g \approx \sqrt{\omega\omega_0}/2$, which is believed to be caused by the precursors of the quantum phase transition [26]. Both in the quantum and semiclassical regime, this transition has been investigated extensively [27,41–44].

Level statistics.—The onset of ergodic behavior is typically diagnosed by inspection of the level spacing distribution [45]. Let $\{E_n\}$ denote the energy levels of the ADM in ascending order. Under the assumption that the density of states equals unity, the distribution $P(s)$ of the level spacings $s_n = E_{n+1} - E_n$ is given by the Poissonian distribution $P(s) = \exp(-s)$ for nonergodic systems following the Berry-Tabor conjecture [46] and the Wigner-Dyson distribution $P(s) = \frac{\pi}{2} s \exp[-(\pi/4)s^2]$ for ergodic systems invariant under orthogonal transformations satisfying the Bohigas-Giannoni-Schmit conjecture [47]. Figure 1 shows the level spacing distribution for the ADM with $\omega = \omega_0$ and $j = 10$ for several values $g_{1,2}$ obtained by exact diagonalization. The ADM is integrable and, hence, nonergodic [13] at $g_1 = 0$ or $g_2 = 0$. One observes that there is an ENET when following the line $g_1 = g_2$, whereas the system remains nonergodic along a line close to the integrable limit $g_1 = 0$, strongly suggesting that the ENET is a consequence of the integrability at $g_1 = 0$ or $g_2 = 0$.

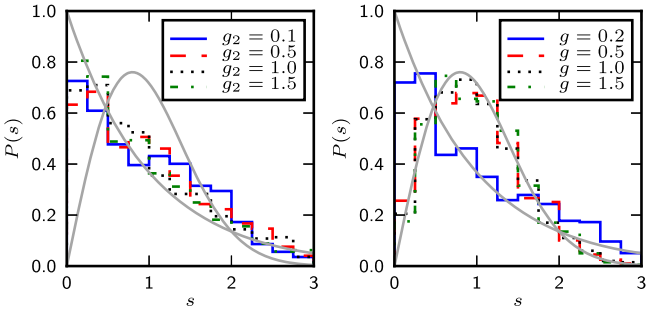

FIG. 1. The normalized distribution of level spacings $s_n = E_{n+1} - E_n$ for the ADM with $\omega = \omega_0 = 1$ and $j = 10$ at $g_1 = 0.1$ (left) and $g = g_1 = g_2$ (right). The histograms are drawn from the sorted energy levels E_n with n ranging from 200 to 1000, where the lowest levels are left out to account for the nonuniform density of states. As a reference, the Poissonian and Wigner-Dyson distributions are shown in gray.

Average ratio of consecutive level spacings.—Aiming to provide a more complete view on where the ENET occurs, we study the average $\langle r\rangle$ over n of the ratio of consecutive level spacings,

$$r_n = \min\left(\frac{s_n}{s_{n-1}}, \frac{s_{n-1}}{s_n}\right), \quad (2)$$

which is independent of the local density of states, and can be used to localize the transition from ergodicity to nonergodicity [48]. The average $\langle r\rangle$ takes a value $\langle r\rangle = 2\ln 2 - 1 \approx 0.386$ for Hamiltonians from the Poissonian ensemble corresponding to the class of nonergodic systems as described above, or a value $\langle r\rangle = 0.5307(1)$ for Hamiltonians from the Gaussian orthogonal ensemble (GOE), corresponding to the above-discussed class of ergodic systems. Figure 2 shows $\langle r\rangle$ for the ADM with $\omega = \omega_0 = 1$ and $j = 10$ as a function of $g_{1,2}$. Clearly, the ENET along the line $g_1 = g_2 = g$ is caused by the integrability of the ADM for $g_1 = 0$ or $g_2 = 0$, and is not related to the precursors of the quantum phase transition at $g_1 + g_2 = 1$ (verified numerically to be close to this line) as it extends over the full ranges $g_1 = 0$ and $g_2 = 0$. One observes that the width of the nonergodic regions on the lower and left sides of the plot increases with increasing values of the coupling parameters, which we expect to be a result of the integrability of the Dicke model in the limit $g/\omega_0 \to \infty$ obtained by rotating $J_x \to J_z$,

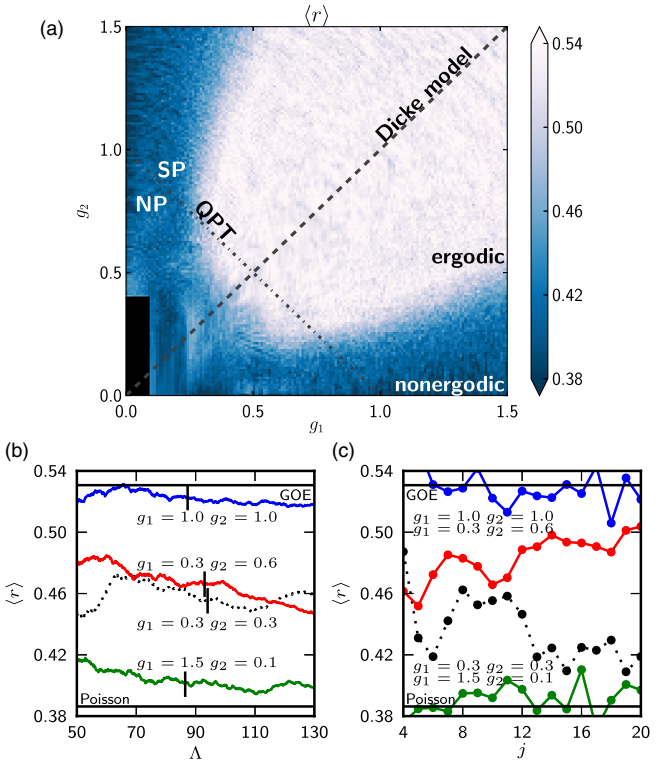

FIG. 2. (a) The average $\langle r\rangle$ of r_n taken over the lowest 1000 energy levels of the ADM with $\omega=\omega_0=1$ and $j=10$ as a function of $g_{1,2}$. The Dicke model and the quantum phase transition (QPT) between the normal (NP) and superradiant (SP) phases are indicated by a dashed and a dash-dotted line, respectively. The lower left-hand corner, where the data artificially suggest nonergodic behavior (see main text), has been masked. (b) The dependence of $\langle r\rangle$ on the upper energy window cutoff Λ for various values $g_{1,2}$. The cutoffs for which the energy windows contain the lowest 1000 energy levels are indicated by black lines. (c) The dependence of $\langle r\rangle$ on j for various values $g_{1,2}$.

$J_z\to J_x$ and translating $a^\dagger\to a^\dagger-2mg/\sqrt{2j}$, where $\omega_0 J_x$ is treated perturbatively. Except for the region around $g_1=g_2\approx 0.3$, there are no qualitative differences when varying the system size or number of energy levels taken into account. For large values of j, the value of $\langle r\rangle$ converges to either the limiting value for ergodic or nonergodic systems, depending on the values of $g_{1,2}$. Expanded up to first order in $g_{1,2}$ around $g_1=g_2=0$, the states $|n,j,m\rangle$ and $|n\pm1,j,m\mp1\rangle$ are near-degenerate with energies for $\omega=\omega_0$ given by $\omega(n+m)$ and $\omega(n+m)\pm g_1\sqrt{j+j^2+m-m^2+2(j+j^2-m^2)n}/\sqrt{2j}$, respectively. This clustering phenomenon with equally separated energy levels leads to a large value of $\langle r\rangle$, artificially suggesting strong nonergodic behavior near $g_1=g_2=0$.

Quantum butterfly effect.—The connection between level statistics and ergodicity is not absolute, and counterexamples do exist [46,49]. Here, we utilize the quantum butterfly effect [50] as an independent dynamical tool to validate the above result. Let $V(t)$ and $W(t)$ denote time-evolving Hermitian operators for which $[V(0),W(0)]=0$ and $[W(0),H]\neq 0$. In an ergodic phase, one expects a small perturbation by applying V at time $t=0$ to strongly affect the outcome of a later measurement of W, thereby contrasting with a nonergodic phase. This effect can be measured by the degree of noncommutativity,

$$F(t)=\frac{1}{2}[\langle V^\dagger(0)W^\dagger(t)V(0)W(t)\rangle_\beta+\text{H.c.}],\qquad(3)$$

written in the Heisenberg picture, with $\langle\mathcal{O}\rangle_\beta$ denoting a thermal average at inverse temperature $\beta=1/T$ in units $k_b=1$ for an operator $\mathcal{O}$ given by $\langle\mathcal{O}\rangle_\beta=\mathrm{Tr}(\mathcal{O}e^{-\beta H})/\mathrm{Tr}(e^{-\beta H})$. Considering, for the moment, the pure state $|\Psi\rangle$ at $t=0$, this effect can be understood by viewing the first term in F (a similar argument holds for the second term) as the overlap between the states $|\Psi_1\rangle=W(t)V(0)|\Psi\rangle$ and $|\Psi_2\rangle=V(0)W(t)|\Psi\rangle$. Since $[V(0),W(0)]=0$, $|\Psi_{1,2}\rangle$ initially fully overlap. With evolving time, the overlap will decrease to a value depending on the size of the accessible Hilbert space in an ergodic phase, thereby contrasting with a nonergodic phase, provided that the perturbation is small. Considering a thermal average, it is expected that $F(t)$ eventually approaches a constant value. Hence, $F(t)$ takes a relatively small or large value in ergodic and nonergodic phases, respectively. The quantum butterfly effect can—in principle—be measured experimentally [51,52]. By adding a probe and control qubit to the system, $|\Psi\rangle$ can be duplicated, after which separate states $W(t)V(0)|\Psi\rangle$ and $V(0)W(t)|\Psi\rangle$ can be obtained by the proper use of entangling gates [53]. Subsequently, the value of $F(t)$ can be obtained by measuring the overlap of these states.

In measuring the quantum butterfly effect in the ADM, we take $W=V$ with $V=a^\dagger a+100$ in the thermal ensemble at inverse temperature β. For the parameters under consideration, the number of bosonic excitations is small compared to 100 (verified numerically), such that V is close to the scaled unit operator, keeping the perturbation small. Figure 3 shows $1-F(t)/F(0)$ for the ADM after equilibration as a function of $g_{1,2}$. This quantity is relatively large (small) in an ergodic (nonergodic) phase. The Dicke model displays a quasi-integrable structure at low energies [27], which is characterized by, e.g., a Poissonian level spacing distribution. Even though part of active research [43,44], the origin of this phenomenon is still unclear. Here, we choose $\beta=1/10$ for which the this low-energy regime does not qualitatively influence the results (verified numerically). One observes qualitative agreement with Fig. 2, showing that the ENET in the ADM is a consequence of the integrability at $g_1=0$ or $g_2=0$. The result is qualitatively independent of variations in the temperature or equilibration time for the wave function to spread out over the full accessible Hilbert space. We also confirm that the ENET

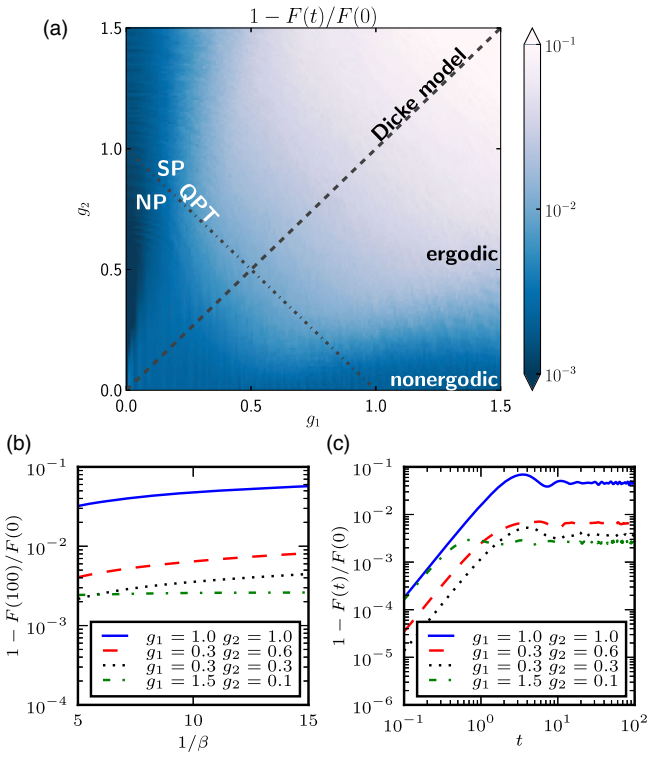

FIG. 3. (a) Density plot of $1-F(t)/F(0)$ at $t=100$ and $\beta=1/10$ for the ADM with $\omega=\omega_0=1$ and $j=5$. Annotations are similar to Fig. 2. Compared to Fig. 2, j is chosen smaller to account for the computational cost of evolving $W(t)$ over time. (b) The temperature dependence of $1-F(100)/F(0)$ for various values $g_{1,2}$. (c) The dependence of $1-F(t)/F(0)$ on time for various values $g_{1,2}$.

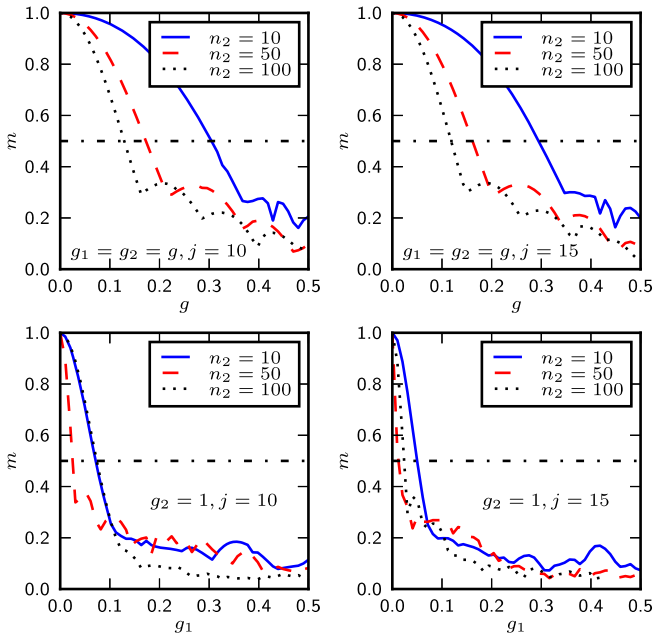

FIG. 4. The quantity m as defined in the main text for the ADM along the line $g_1=g_2=g$ ($g_1=1$) with $g=0$ ($g_2=0$) denoting the integrable Hamiltonian in the upper (lower) part. The results are shown for system size $j=10$ (left) and $j=15$ (right).

is unrelated to the precursors of the normal-superradiant quantum phase transition.

Discussion.—In addition to the diagnostics for ergodicity utilized in this Letter, multiple alternative measures exist. Let $H(\lambda)$ denote a parameter-dependent Hamiltonian, and suppose $H(\lambda_1)$ is integrable, opposed to $H(\lambda_2)$. Reference [16] argues that $H(\lambda_2)$ is nonergodic if for any eigenstate $|n_2\rangle$ there is an eigenstate $|n_1\rangle$ of $H(\lambda_1)$ such that $|\langle n_1|n_2\rangle|^2 > 1/2$. Here, we investigate this proposal by determining the quantity $m=\max_i|\langle i|n_2\rangle|^2$ with $|i\rangle$ running over all eigenstates of the integrable Hamiltonian and $|n_2\rangle$ denoting the n_2th eigenstate of the nonintegrable Hamiltonian labeled according to the corresponding eigenvalues in ascending order. Figure 4 shows m for the ADM with $g_1=g_2=0$ (upper part) and $g_1=0$, $g_2=1$ (lower part) as the integrable Hamiltonian for several eigenvectors and system sizes as a function of $g=g_1=g_2$ and g_1, respectively. Opposed to the results above, this measure suggests that the ENET moves towards the integrable regime $g_1=0$ or $g_2=0$ with an increasing energy scale or system size j. We believe that future studies focusing on this discrepancy would be helpful.

Conclusions.—We have shown that the ergodic-nonergodic transition in the Dicke model is a result of integrability of the anisotropic Dicke model when setting one of the coupling constants to zero. We have shown that there is an extended nonergodic region, which can be considered as a hint for the existence of a still elusive quantum version of the Kolmogorov-Arnold-Moser theorem. Similar observations have been made for, e.g., Gaudin models [17], spinless fermion models [3], or one-dimensional Bose gases [18]. Experimental setups feasible to verify the results experimentally have been proposed [20]. We have used both the level spacing distribution and the average ratio of consecutive level spacings as static and the quantum butterfly effect as dynamical probes for ergodicity. In addition, we have shown that there is no intrinsic relation between the ergodic-nonergodic transition and the precursors of the normal-superradiant quantum phase transition. We expect that a similar approach as used in this Letter can be used to find extended nonergodic phases in other quantum many-body systems, such as disordered spin chains.

The work of W. B. and V. G. is part of the Delta-ITP consortium, a program of the Netherlands Organization for Scientific Research (NWO) that is funded by the Dutch Ministry of Education, Culture and Science (OCW).

*w.buijsman@uva.nl

[1] M. Rigol, Breakdown of Thermalization in Finite One-Dimensional Systems, Phys. Rev. Lett. **103**, 100403 (2009).

[2] A. Pal and D. A. Huse, Many-body localization phase transition, Phys. Rev. B **82**, 174411 (2010).

[3] B. Bertini, F. H. L. Essler, S. Groha, and N. J. Robinson, Prethermalization and Thermalization in Models with Weak Integrability Breaking, Phys. Rev. Lett. **115**, 180601 (2015).

[4] O. Giraud and I. García-Mata, Average diagonal entropy in nonequilibrium isolated quantum systems, Phys. Rev. E **94**, 012122 (2016).

[5] R. Orbach, Linear antiferromagnetic chain with anisotropic coupling, Phys. Rev. **112**, 309 (1958).

[6] F. Essler, H. Frahm, F. Gömann, A. Klümper, and V. Korepin, *The One-Dimensional Hubbard Model* (Cambridge University Press, Cambridge, England, 2005).

[7] A. V. Khaetskii, D. Loss, and L. Glazman, Electron Spin Decoherence in Quantum Dots due to Interaction with Nuclei, Phys. Rev. Lett. **88**, 186802 (2002).

[8] M. A. Cazalilla, R. Citro, T. Giamarchi, E. Orignac, and M. Rigol, One dimensional bosons: From condensed matter systems to ultracold gases, Rev. Mod. Phys. **83**, 1405 (2011).

[9] T. Giamarchi, *Quantum Physics in One Dimension*, 1st ed. (Oxford University Press, Oxford, England, 2003).

[10] J. Z. Imbrie, Diagonalization and Many-Body Localization for a Disordered Quantum Spin Chain, Phys. Rev. Lett. **117**, 027201 (2016).

[11] F. Bagnoli, F. Cecconi, A. Flammini, and A. Vespignani, Short-period attractors and non-ergodic behavior in the deterministic fixed-energy sandpile model, Europhys. Lett. **63**, 512 (2003).

[12] G. Drótos, T. Bódai, and T. Tél, Quantifying nonergodicity in nonautonomous dissipative dynamical systems: An application to climate change, Phys. Rev. E **94**, 022214 (2016).

[13] M. Srednicki, Chaos and quantum thermalization, Phys. Rev. E **50**, 888 (1994).

[14] A. Kolmogorov, On conservation of conditionally periodic motions for a small change in Hamilton's function (in Russian), Dokl. Akad. Nauk SSSR **98**, 527 (1954).

[15] V. Arnold, *Mathematical Methods of Classical Mechanics*, 2nd ed. (Springer Science, Business, Media, New York, 1989).

[16] G. Hose and H. S. Taylor, Quantum Kolmogorov-Arnol'd-Moser-like Theorem: Fundamentals of Localization in Quantum Theory, Phys. Rev. Lett. **51**, 947 (1983).

[17] P. Barmettler, D. Fioretto, and V. Gritsev, Non-equilibrium dynamics of Gaudin models, Europhys. Lett. **104**, 10004 (2013).

[18] G. P. Brandino, J.-S. Caux, and R. M. Konik, Glimmers of a Quantum Kam Theorem: Insights from Quantum Quenches in One-Dimensional Bose Gases, Phys. Rev. X **5**, 041043 (2015).

[19] R. H. Dicke, Coherence in spontaneous radiation processes, Phys. Rev. **93**, 99 (1954).

[20] F. Dimer, B. Estienne, A. S. Parkins, and H. J. Carmichael, Proposed realization of the Dicke-model quantum phase transition in an optical cavity QED system, Phys. Rev. A **75**, 013804 (2007).

[21] M. Tomka, M. Pletyukhov, and V. Gritsev, Supersymmetry in quantum optics and in spin-orbit coupled systems, Sci. Rep. **5**, 13097 (2015).

[22] M. Gaudin, Diagonalisation d'une classe d'Hamiltoniens de spin, J. Phys. (Paris) **37**, 1087 (1976).

[23] K. Baumann, C. Guerlin, F. Brennecke, and T. Esslinger, Dicke quantum phase transition with a superfluid gas in an optical cavity, Nature (London) **464**, 1301 (2010).

[24] M. P. Baden, K. J. Arnold, A. L. Grimsmo, S. Parkins, and M. D. Barrett, Realization of the Dicke Model Using Cavity-Assisted Raman Transitions, Phys. Rev. Lett. **113**, 020408 (2014).

[25] Y. K. Wang and F. T. Hioe, Phase transition in the Dicke model of superradiance, Phys. Rev. A **7**, 831 (1973).

[26] C. Emary and T. Brandes, Quantum Chaos Triggered by Precursors of a Quantum Phase Transition: The Dicke Model, Phys. Rev. Lett. **90**, 044101 (2003); Chaos and the quantum phase transition in the Dicke model, Phys. Rev. E **67**, 066203 (2003).

[27] P. Pérez-Fernández, A. Relaño, J. M. Arias, P. Cejnar, J. Dukelsky, and J. E. García-Ramos, Excited-state phase transition and onset of chaos in quantum optical models, Phys. Rev. E **83**, 046208 (2011).

[28] C. M. Lóbez and A. Relaño, Entropy, chaos, and excited-state quantum phase transitions in the Dicke model, Phys. Rev. E **94**, 012140 (2016).

[29] L. Song, D. Yan, J. Ma, and X. Wang, Spin squeezing as an indicator of quantum chaos in the Dicke model, Phys. Rev. E **79**, 046220 (2009).

[30] P. Giorda and P. Zanardi, Quantum chaos and operator fidelity metric, Phys. Rev. E **81**, 017203 (2010).

[31] D. A. Wisniacki and A. J. Roncaglia, Sensitivity to perturbations and quantum phase transitions, Phys. Rev. E **87**, 050902 (2013).

[32] S. H. Shenker and D. Stanford, Black holes and the butterfly effect, J. High Energy Phys. 03 (2014) 067.

[33] S. H. Shenker and D. Stanford, Stringy effects in scrambling, J. High Energy Phys. 05 (2015) 132.

[34] P. Hosur, X.-L. Qi, D. A. Roberts, and B. Yoshida, Chaos in quantum channels, J. High Energy Phys. 02 (2016) 004.

[35] W. Fu and S. Sachdev, Numerical study of fermion and boson models with infinite-range random interactions, Phys. Rev. B **94**, 035135 (2016).

[36] D. A. Roberts and B. Swingle, Lieb-Robinson Bound and the Butterfly Effect in Quantum Field Theories, Phys. Rev. Lett. **117**, 091602 (2016).

[37] X. Chen, T. Zhou, D. A. Huse, and E. Fradkin, Out-of-time-order correlations in many-body localized and thermal phases, Ann. Phys. (Berlin), DOI: 10.1002/andp.201600332 (2016).

[38] L. J. Zou, D. Marcos, S. Diehl, S. Putz, J. Schmiedmayer, J. Majer, and P. Rabl, Implementation of the Dicke Lattice Model in Hybrid Quantum System Arrays, Phys. Rev. Lett. **113**, 023603 (2014).

[39] W.-l. Song, W.-l. Yang, Z.-q. Yin, C.-y. Chen, and M. Feng, Controllable quantum dynamics of inhomogeneous nitrogen-vacancy center ensembles coupled to superconducting resonators, Sci. Rep. **6**, 33271 (2016).

[40] F. T. Hioe, Phase transitions in some generalized Dicke models of superradiance, Phys. Rev. A **8**, 1440 (1973).

[41] A. Altland and F. Haake, Quantum Chaos and Effective Thermalization, Phys. Rev. Lett. **108**, 073601 (2012).

[42] A. Altland and F. Haake, Equilibration and macroscopic quantum fluctuations in the Dicke model, New J. Phys. **14**, 073011 (2012).

[43] T. Brandes, Excited-state quantum phase transitions in Dicke superradiance models, Phys. Rev. E **88**, 032133 (2013).

[44] J. Chávez-Carlos, M. A. Bastarrachea-Magnani, S. Lerma-Hernández, and J. G. Hirsch, Classical chaos in atom-field systems, Phys. Rev. E **94**, 022209 (2016).

[45] H.-J. Stöckmann, *Quantum Chaos, An Introduction* (Cambridge University Press, Cambridge, England, 1999).

[46] M. Berry and M. Tabor, Level clustering in the regular spectrum, Proc. R. Soc. A **356**, 375 (1977).

[47] O. Bohigas, M. J. Giannoni, and C. Schmit, Characterization of Chaotic Quantum Spectra and Universality of Level Fluctuation Laws, Phys. Rev. Lett. **52**, 1 (1984).

[48] Y. Y. Atas, E. Bogomolny, O. Giraud, and G. Roux, Distribution of the Ratio of Consecutive Level Spacings in Random Matrix Ensembles, Phys. Rev. Lett. **110**, 084101 (2013).

[49] F. Finkel and A. González-López, Global properties of the spectrum of the Haldane-Shastry spin chain, Phys. Rev. B **72**, 174411 (2005).

[50] D. A. Roberts and D. Stanford, Diagnosing Chaos Using Four-Point Functions in Two-Dimensional Conformal Field Theory, Phys. Rev. Lett. **115**, 131603 (2015).

[51] B. Swingle, G. Bentsen, M. Schleier-Smith, and P. Hayden, Measuring the scrambling of quantum information, Phys. Rev. A **94**, 040302 (2016).

[52] G. Zhu, M. Hafezi, and T. Grover, Measurement of many-body chaos using a quantum clock, Phys. Rev. A **94**, 062329 (2016).

[53] J. S. Pedernales, R. Di Candia, I. L. Egusquiza, J. Casanova, and E. Solano, Efficient Quantum Algorithm for Computing n-Time Correlation Functions, Phys. Rev. Lett. **113**, 020505 (2014).